

Supernova SN 2020faa - an iPTF14hls look-alike?

S. Yang[1], J. Sollerman[1], L. ist to be completed and ordered.[2], D. A. Perley[3], A. Horesh[4], R. Lunnan[1], P. Nugent[5,6], S. Schulze[7], N. Strotjohann[7], T. Kupfer[8], F. J. Masci[9], R. Riddle[10], B. Rusholme[9], and Y. Sharma[10]

[1] Department of Astronomy, The Oskar Klein Center, Stockholm University, AlbaNova, 10691 Stockholm, Sweden
[2] Partner institutions
[3] Astrophysics Research Institute, Liverpool John Moores University, IC2, Liverpool Science Park, 146 Brownlow Hill, Liverpool L3 5RF, UK
[4] Racah Institute of Physics, The Hebrew University of Jerusalem, Jerusalem 91904, Israel
[5] Lawrence Berkeley National Laboratory, 1 Cyclotron Road, Berkeley, CA 94720, USA
[6] Department of Astronomy, University of California, Berkeley, CA 94720-3411, USA
[7] Department of Particle Physics and Astrophysics, Weizmann Institute of Science, 234 Herzl St, 76100 Rehovot, Israel
[8] Texas Tech University, Department of Physics & Astronomy, Box 41051, 79409, Lubbock, TX, USA
[9] IPAC, California Institute of Technology, 1200 E. California, Blvd, Pasadena, CA 91125, USA
[10] Caltech Optical Observatories, California Institute of Technology, Pasadena, CA 91125, USA

September 3, 2020

ABSTRACT

Context. We present observations of SN 2020faa (ZTF20aatqesi). This Type II supernova (SN) displays a luminous light curve that from an initial decline started to rebrighten. We investigate this in relation to the famous supernova iPTF14hls, which received a lot of attention and multiple interpretations in the literature.

Aims. We demonstrate the great similarity between SN 2020faa and iPTF14hls during the first 6 months, and use this both to forecast the evolution of SN 2020faa and to reflect on the less well observed early evolution of iPTF14hls.

Methods. We present and analyse our observational data, consisting mainly of optical light curves from the Zwicky Transient Facility in gri as well as a sequence of optical spectra. We construct color curves, a bolometric light curve, compare ejecta-velocity and Black-body radius evolutions for the two supernovae, as well as for more typical Type II SNe.

Results. The light curves show a great similarity with those of iPTF14hls over the first 6 months, in luminosity, timescale and colors. Also the spectral evolution of SN 2020faa is that of a Type II SN, although it probes earlier epochs than what was available for iPTF14hls.

Conclusions. The similar light curve behaviour is suggestive of SN 2020faa being a new iPTF14hls. We present these observations now to advocate follow-up observations, since most of the more striking evolution of SN iPTF14hls came later, with LC undulations and a spectacular long-livety. On the other hand, for SN 2020faa we have better constraints on the explosion epoch than we had for iPTF14hls, and we have been able to spectroscopically monitor it from earlier phases than was done for the more famous sibling.

Key words. supernovae: general – supernovae: individual: SN 2020faa, ZTF20aatqesi, iPTF14hls

1. Introduction

The extraordinary supernova (SN) iPTF14hls was a Type II supernova (SN II), first reported by Arcavi et al. (2017, hereafter A17) as having a long-lived (600+ d) and luminous light curve (LC) showing at least five episodes of rebrightening. Sollerman et al. (2019, hereafter S19) followed the supernova until 1000 days when it finally faded from visibility.

The spectra of iPTF14hls were similar to those of other hydrogen-rich supernovae (SNe), but evolved at a slower pace. A17 described a scenario where this could be the explosion of a very massive star that ejected a huge amount of mass prior to explosion. They connect such eruptions with the pulsational pair-instability mechanism.

Following the report of A17, a large number of interpretations were suggested for this unusual object. These covered a wide range of progenitors and powering mechanism. For example, Chugai (2018) agreed on the massive ejection scenario, while Andrews & Smith (2018) argued for interaction with the circumstellar medium (CSM) as the source for the multiple rebrightenings in the LC, which was supported by S19. Dessart (2018) instead suggested a magnetar as the powering mechanism, whereas Soker & Gilkis (2017) advocate a common-envelope jet. Wang et al. (2018) proposed a fall-back accretion model for iPTF14hls and Woosley (2018) discuss pros and cons of several of the above-mentioned models, and whether the event was indeed a final explosion. Moriya et al. (2019) interpret the phenomenon as a wind from a very massive star.

Taken together, this suite of publications demonstrate how extreme objects like iPTF14hls challenge most theoretical models and forces us to expand the frameworks for transient phenomena. But iPTF14hls was a single specimen - until now.

In this paper, we present observations of SN 2020faa (ZTF20aatqesi), a Type II supernova that observationally appears to be similar to iPTF14hls during the first six months. We present light curves and spectra to highlight this similarity and also add information that was not available for iPTF14hls, like earlier spectroscopy and better constrains on the explosion epoch. In addition to the ground-based data, we have a few epochs of *Neil Gehrels Swift Observatory* (*Swift*, Gehrels et al. 2004) observations. The main aim of this paper is to direct the attention of the community to this transient, which may - or may not - evolve in the same extraordinary way as did iPTF14hls.

The paper is structured as follows. In Sect. 2, we outline the detection and classification of SN 2020faa in Sect. 2.1, the ground-based optical SN imaging observations and the corresponding data reductions are presented in Sect. 2.2, whereas in Sect. 2.3 we describe the *Swift* observations. A search for a precursor is done in Sect. 2.4, a discussion on its host galaxy is provided in Sect. 2.6, and the optical spectroscopic follow-up campaign is presented in Sect. 2.5. An analysis and discussion of the results is given in Sect. 3 and this is summarised in Sect. 4.

For iPTF14hls, we follow A17 and adopt a redshift of $z = 0.0344$, corresponding to a luminosity distance of 156 Mpc. We correct all photometry for Milky Way (MW) extinction, $E(B-V) = 0.014$ mag, but make no correction for host-galaxy extinction. For SN 2020faa, we use $z = 0.04106$ (see below), corresponding to a luminosity distance of 187 Mpc (distance modulus 36.36 mag) using the same cosmology as A17. The MW extinction is $E(B-V) = 0.022$ mag, and also in this case we adopt no host galaxy extinction. We follow A17 and use the PTF discovery date as a reference epoch for all phases for iPTF14hls, while for SN 2020faa, we set the first ATLAS detection date as reference epoch.

2. Observations and Data reduction

2.1. Detection and classification

The first detection of SN 2020faa (a.k.a. ZTF20aatqesi) with the Palomar Schmidt 48-inch (P48) Samuel Oschin telescope was on 2020 March 28 (JD = 2458936.8005), as part of the Zwicky Transient Facility (ZTF) survey (Bellm et al. 2019; Graham et al. 2019). The object had then already been discovered and reported to the Transient Name Server (TNS[1]) by the ATLAS collaboration (Tonry et al. 2020) with a discovery date of March 24 ($\mathrm{JD_{discovery}} = 2458933.104$) at 18.28 mag in the cyan band, and a reported last non-detection (> 18.57) 14 days before discovery.

The first ZTF detection was made in the g band, with a host-subtracted magnitude of 18.40 ± 0.09 mag, at the J2000.0 coordinates $\alpha = 14^h47^m09.50^s$, $\delta = +72°44'11.5''$. The first r-band detection came in 3.6 hours later at 18.50 ± 0.10. The non-detections from ZTF include a g-band non-detection from 15 days before discovery, but this is a shallow global limit (> 17.46), whereas the one at 17 days before discovery is deeper at > 19.37 mag. The constraints on the time of explosion for SN 2020faa are thus not fantastic, but in comparison with the very large uncertainty for iPTF14hls (∼ 100 days) they are quite useful.

SN 2020faa is positioned in the edge on spiral galaxy WISEA J144709.05+724415.5 which did not have a reported redshift in the NED catalog, although the CLU catalog has it listed as CLU J144709.1+724414 at the same redshift as our spectroscopy provides below. The supernova together with the host galaxy and the field of view is shown in Fig. 1.

SN 2020faa was classified as a Type II SN (Perley et al. 2020) based on a spectrum obtained on 2020 April 6 with the Liverpool telescope (LT) equipped with the SPRAT spectrograph. That spectrum revealed broad Hα and Hβ in emission, the blue edge being shifted by ∼ 8000 km s^{-1} with respect to the narrow emission line from the galaxy that provided the redshift $z = 0.041$ consistent with CLU as mentioned above. The LT spectrum confirmed the tentative redshift and classification deduced from our first spectrum, obtained with the Palomar 60-inch telescope (P60; Cenko et al. 2006) equipped with the Spectral Energy Distribution Machine (SEDM; Blagorodnova et al. 2018). That first spectrum was taken already on March 31, but the quality was not good enough to warrant a secure classification.

2.2. Optical photometry

Following the discovery, we obtained regular follow-up photometry during the slowly declining phase in g, r and i bands with the ZTF camera (Dekany et al. 2020) on the P48. This first decline lasted for ∼ 50 days, and no further attention was given to the SN during this time.

Later on, after rebrightening started, we also obtained a few epochs of triggered photometry in gri with the SEDM on the P60. The light curves from the P48 come from the ZTF pipeline (Masci et al. 2019). Photometry from the P60 were produced with the image-subtraction pipeline described in Fremling et al. (2016), with template images from the Sloan Digital Sky Survey (SDSS; Ahn et al. 2014). This pipeline produces PSF magnitudes, calibrated against SDSS stars in the field. All magnitudes are reported in the AB system.

The reddening corrections are applied using the Cardelli et al. (1989) extinction law with $R_V = 3.1$. No further host galaxy extinction has been applied, since there is no sign of any Na I D absorption in our spectra. The light curves are shown in Fig. 2.

After the initial decline of about 50 days (this is past discovery in the observer's frame), SN 2020faa started to slowly brighten again. This continued for about 70 days and happened in all three bands. Once this was realized in late May 2020, a more intense follow-up could be activated, in particular with regular spectroscopic observations (Sect. 2.5.)

We used a Gaussian Processing (GP) algorithm[2], to quantify the numbers and found that the peak happened at $\mathrm{m}_r^{\mathrm{peak}} = 17.49 \pm 0.01$ after $\mathrm{t}^r_{\mathrm{rise}} = 114.51 \pm 0.10$ rest frame days, via $scipy.find\_peaks$. In the g and i bands the photometric behavior follows the same trend, and peaked at $\mathrm{m}_g^{\mathrm{peak}} = 17.83$ after $\mathrm{t}^g_{\mathrm{rise}} = 114.70$ as well as $\mathrm{m}_i^{\mathrm{peak}} = 17.58$ after $\mathrm{t}^i_{\mathrm{rise}} = 119.70$ rest frame days.

2.3. Swift-observations

2.3.1. UVOT photometry

A series of ultraviolet (UV) and optical photometry observations were obtained with the UV Optical Telescope onboard the Neil Gehrels *Swift* observatory (UVOT; Gehrels et al. 2004; Roming et al. 2005).

Our first *Swift*/UVOT observation was performed on 2020 Jul 03 (JD = 2459034.4226) and provided detections in all the bands. However, upon inspection it is difficult to assess to what extent the emission is actually from the supernova itself, or if it is diffuse emission from the surroundings. We would need to await template subtracted images to get reliable photometry.

2.3.2. X-rays

With *Swift* we also used the onboard X-Ray Telescope (XRT; Burrows et al. 2006). We analysed all data with the online-tools of the UK *Swift* team[3] that use the methods described in Evans

[1] https://wis-tns.weizmann.ac.il/

[2] https://george.readthedocs.io

[3] https://www.swift.ac.uk/user_objects

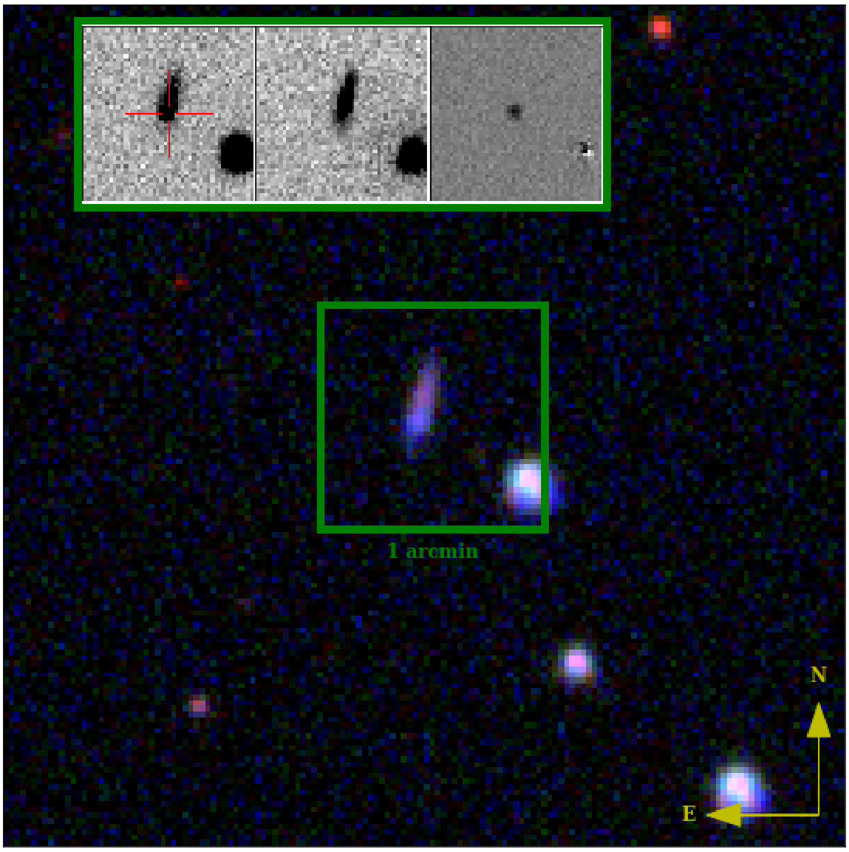

Fig. 1 A *gri*-colour composite image of SN 2020faa and its environment, as observed with the P48 telescope on 2020 April 5, +8 days after first the ZTF detection. The *g*-band image subtraction is shown in the top panel.

et al. (2007) and Evans et al. (2009) and the software package HEASoft[4] version 6.26.1 to search for X-ray emission at the location of SN 2020ffa.

Combining the five epochs taken in July 2020 amounts to a total XRT exposure time of $\lesssim$ 11000 s ($\lesssim$ 3 hr), and provides a 3σ upper limit of 0.001 count s^{-1} between 0.3 and 10 keV. If we assume a power-law spectrum with a photon index of $\Gamma = 2$ and a Galactic hydrogen column density of 2.65×10^{20} cm^{-2} (HI4PI Collaboration et al. 2016) this would correspond to an unabsorbed 0.3–10.0 keV flux of 4×10^{-14} erg cm^{-2} s^{-1}. At the luminosity distance of SN 2020ffa this corresponds to a luminosity of less than $L_X = 2 \times 10^{41}$ erg s^{-1} (0.3–10 keV) at an epoch of $\sim$ 103 days rest-frame days since discovery.

2.4. Pre-discovery imaging

A particular peculiarity for iPTF14hls was the tentative detection of a precursor in images taken long before the discovery of the transient, from the year 1954. We therefore looked at the P48 imaging of the field of SN 2020faa for some epochs prior to discovery, both by ZTF and by the predeccesor PTF. For the PTF images, image subtraction revealed no detection (5σ) for the 65 *r*-band images obtained between May 9, 2009 and July 24, 2010. For ZTF, we searched for pre-explosion outbursts in 1538 observations that were obtained in the *g*, *r* and *i* band in the 2.3 years before the first detection of SN 2020faa. No outbursts are detected when searching unbinned or binned (1 to 90-day long bins) light curves following the methods described by Strotjohann et al. (in prep.), see Fig.3. The precursor detected prior to iPTF14hls had an absolute *r*-band magnitude of −15.6 and we can rule out as bright outbursts for 50% of the time assuming that an outburst lasts for at least one week.

2.5. Optical spectroscopy

Spectroscopic follow-up was conducted with SEDM mounted on the P60. Further spectra were obtained with the Nordic Optical Telescope (NOT) using the A. Faint Object Spectrograph (ALFOSC). A log of the spectral observations is provided in Table 1, which includes 12 epochs of spectroscopy. SEDM spec-

[4] https://heasarc.gsfc.nasa.gov/docs/software/heasoft

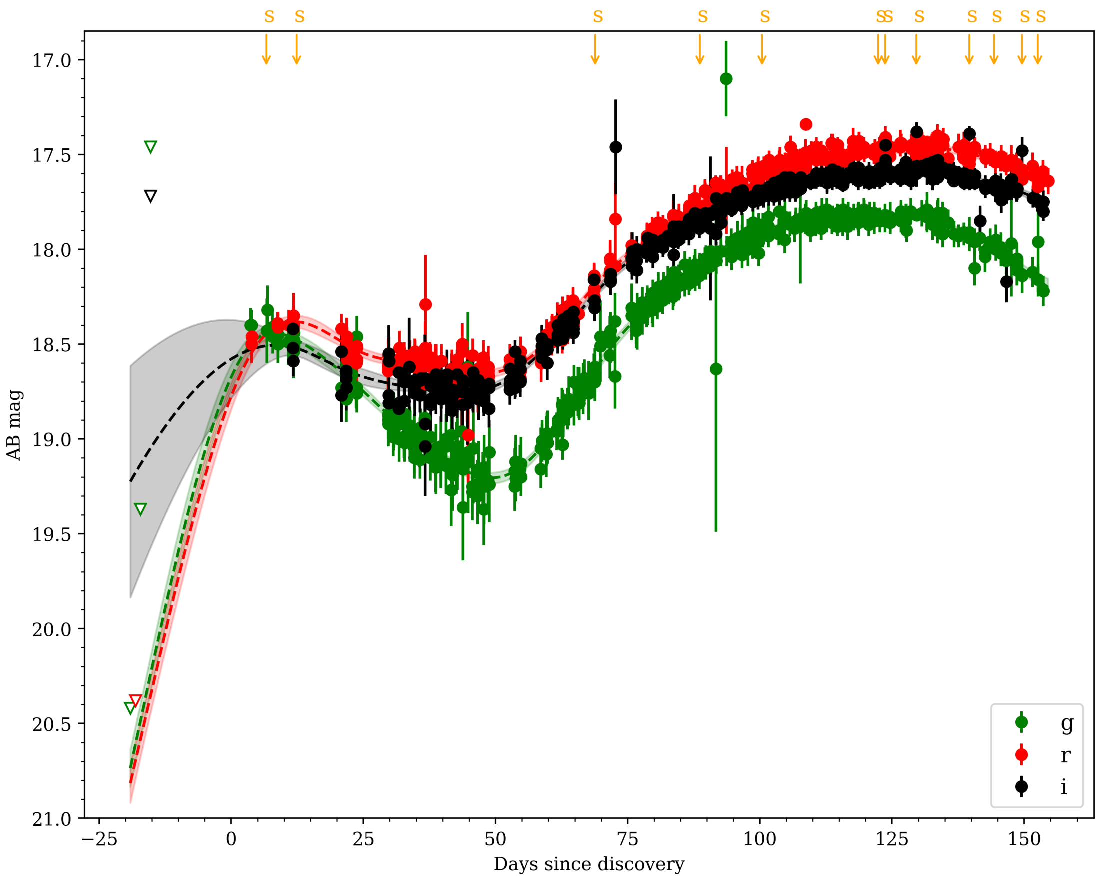

Fig. 2 Light curves of SN 2020faa in g (green symbols), r (red) band and i (black) band. These are observed (AB) magnitudes plotted versus observer frame time in days since discovery. The yellow arrows on top indicate the epochs of spectroscopy, and the dashed lines with error regions are Gaussian Process estimates of the interpolated LC. Relevant upper limits are selected to constrain the early phase of the LC, shown as inverted triangles.

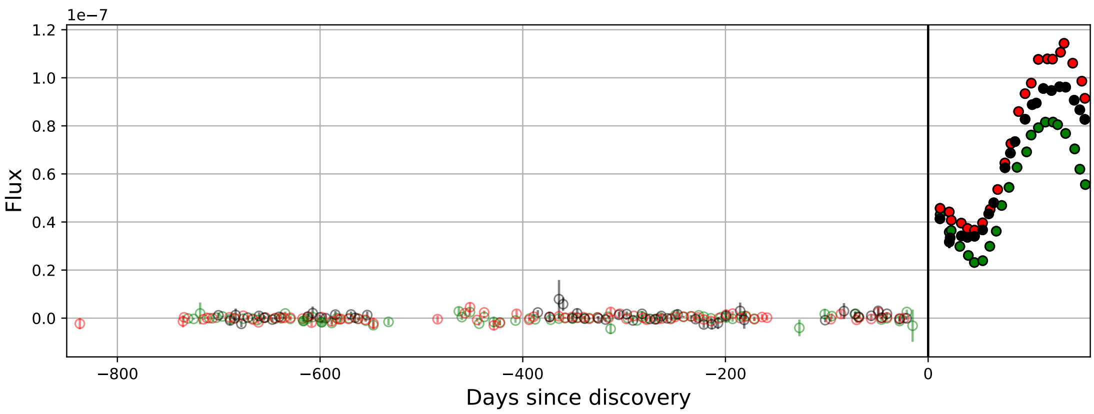

Fig. 3 Pre-explosion images in ZTF for SN 2020faa reveal no precursos in g (green symbols), r (red) band or i (black) bands. The flux f is given as a dimensionless ratio and can be converted via $m_{AB} = -2.5 \log_{10}(f)$. Filled data points are $\gtrsim 5\sigma$ detections, whereas shaded points are between 3 and 5 sigma and open symbols are less significant than 3 sigma.

tra were reduced using the pipeline described by Rigault et al. (2019) and the spectra from La Palma were reduced using standard pipelines. The spectra were finally absolute calibrated using the GP interpolated measured magnitudes and then corrected for MW extinction. All spectral data and corresponding information will be made available via WISeREP[5] (Yaron & Gal-Yam 2012).

[5] https://wiserep.weizmann.ac.il

2.6. Host galaxy

2.6.1. Photometry

We retrieved science-ready coadded images from the *Galaxy Evolution Explorer* (*GALEX*) general release 6/7 (Martin et al. 2005), the Panoramic Survey Telescope and Rapid Response System (Pan-STARRS, PS1) Data Release 1 (Chambers et al. 2016), the Two Micron All Sky Survey (2MASS; Skrutskie et al. 2006), and preprocessed *WISE* images (Wright et al. 2010) from the unWISE archive (Lang 2014)[6]. The unWISE images are based on the public *WISE* data and include images from the ongoing NEOWISE-Reactivation mission R3 (Mainzer et al. 2014; Meisner et al. 2017).

We measured the brightness of the host in a consistent way from the far-ultraviolet to the mid-infrared (i.e., measuring the total flux and preserving the instrinsic galaxy colours) using LAMBDAR[7] (Lambda Adaptive Multi-Band Deblending Algorithm in R; Wright et al. 2016) and the methods described in Schulze et al. (2020). Table 2 gives the measurements in the different bands.

2.6.2. Spectral energy distribution modelling

We modelled the spectral energy distribution with the software package prospector version 0.3 (Leja et al. 2017). Prospector uses the Flexible Stellar Population Synthesis (FSPS) code (Conroy et al. 2009) to generate the underlying physical model and python-fsps (Foreman-Mackey et al. 2014) to interface with FSPS in python. The FSPS code also accounts for the contribution from the diffuse gas (e.g., HII regions) based on the Cloudy models from Byler et al. (2017). Furthermore, we assumed a Chabrier initial mass function (Chabrier 2003) and approximated the star formation history (SFH) by a linearly increasing SFH at early times followed by an exponential decline at late times (functional form $t \times \exp(-t/\tau)$). The model was attenuated with the Calzetti et al. (2000) model. Finally, we use the dynamic nested sampling package dynesty (Speagle 2020) to sample the posterior probability function.

3. Analysis and Discussion

The LCs in the different bands are presented in Sect. 3.1, and Sect. 3.2 presents our series of SN spectra. In Sect. 3.3 we outline how the bolometric light curve was constructed from the multiband data. The data are analysed in conjunction with the data of iPTF14hls presented by S19, and some specific normal Type II SNe.

3.1. Light curves

The g-, $r-$ and i-band LCs of our SN are displayed in Fig. 2. The general behaviour of the LCs was already discussed in Sect. 2.2, and the main characteristic is of course the slow evolution with the initial decline followed by the late rise over several months. In the figure we have also included the most restricting upper limits as triangles (5σ), while the arrows on top of the figure illustrate epochs of spectroscopy. The Gaussian Process (GP) interpolation is also shown, which is used to for absolute calibrating the spectra. For the GP, we perform time series forecasting for the joint multi-band fluxes with their corresponding central wavelengths, in order to include color information. In this work, we use a flat mean function and a stationary kernel `Matern 3/2` for the form.

In Fig. 4 we show the $g-$, $r-$ and $i-$band light curves in absolute magnitudes together with the light curves of iPTF14hls from S19. The bottom left has an inset highlighting the first 200 days, which zoom in on the evolution of SN 2020faa. The magnitudes in Fig. 4 are in the AB system and have been corrected for distance modulus and MW extinction, and are plotted versus rest frame days past discovery.

The inset shows the remarkable similarity in absolute magnitude and timescale of the two SNe, whereas the full figure might be seen as a prediction for the future evolution of SN 2020faa. We will continue to follow the SN at best effort with ZTF, but report on these results already now to encourage the community to keep an eye on the continued evolution of this transient. We note that with a declination of +72 degrees the source is well placed to be observed around the year from Northern observatories. No offset was applied to match the absolute magnitudes, they fall very well on top of each other anyway. Note that also no shift was applied in the time scales, we have plotted iPTF14hls since time of discovery, which supports a similar evolution also in this dimension. It is worth to note that the explosion date[8] for iPTF14hls was unconstrained by several months (A17), which made it more difficult to estimate for example total radiated energy for that SN. The comparison here makes it likely that it was not discovered very late after all.

Needless to say, the evolution is very different from that of normal SNe Type II, which was already demonstrated by the comparison to SN 1999em (A17, their fig. 1). Such a supernova normally stays on a relative flat plateau for about 100 days, and then quickly plummets to the radioactive decay tail. The rejuvenated long-timescale rise for SN 2020faa argues, as for iPTF14hls, that a different powering mechanism must be at play.

The color evolution of SN 2020faa is shown in Fig. 5. We plot $g - r$ in the upper panel and $r - i$ in the lower panel, both corrected for MW extinction. In doing this, no interpolation was used. Given the excellent light curve sampling we used only data where the pass band magnitudes were closer in time than 0.1 days. Comparison is made with the color evolution for iPTF14hls, but this SN was not covered at early phases. There is anyway evidence for similar colors, which argue against significant host extinction. We also compare the colors against some more normal Type II SNe, i.e. 2013am (Tomasella et al. 2018), 2013fs (Yaron et al. 2017) and 2013ej (Valenti et al. 2013; Bose et al. 2015; Huang et al. 2015; Dhungana et al. 2016; Mauerhan et al. 2017), which are selected from de Jaeger et al. (2018) without host extinction correction on photometry.

3.2. Spectra

The log of spectroscopic observations was provided in Table 1 and the sequence of spectra is shown in Fig. 6. Overall, these are spectra of a typical Type II SN. We compare these with spectra from iPTF14hls. Note that the rise of iPTF14hls was not picked up immediately and therefore the first spectrum of that supernova was only obtained more than 100 days past first detection. We were somewhat faster for SN 2020faa, and can measure the evolution of the expansion velocity from 65 days past discovery.

These velocities are shown in Fig. 8, where we compare to iPTF14hls and to SN 1999em following the methodology of A17, see their fig. 3. We measured the velocities for SN 2020faa

[6] http://unwise.me
[7] https://github.com/AngusWright/LAMBDAR
[8] or maybe better, time of first light.

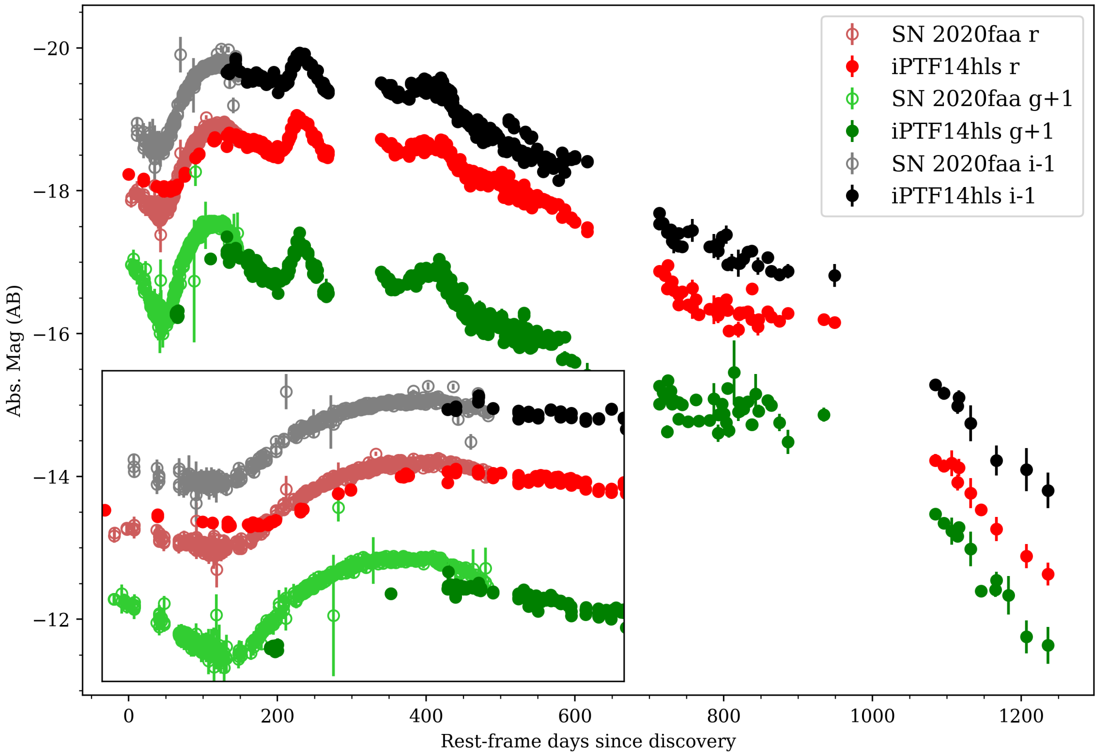

Fig. 4 Absolute magnitudes of SN 2020faa together with the light curves of iPTF14hls. No scaling has been applied to match these SNe. The inset highlights the early evolution (exactly 200 days), which is where SN 2020faa demonstrates a striking similarity with the early iPTF14hls light curves.

using `iraf` to fit a Gaussian to the minimum of the absorption lines. The time evolution of the velocities measured for Hα, Hβ and for Fe ii λ5169 match very well with those of iPTF14hls at the common epochs, but also extend to earlier phases. The velocities for the comparison SNe are taken from A17. The striking characteristic of the time evolution for iPTF14hls was the very flat velocity evolution. We do not know (yet) if SN 2020faa will follow such a flat evolution, or if iPTF14hls had a faster evolution in the first 100 days.

For iPTF14hls, the complete spectral evolution was also slow. We followed the approach in A17 and used superfit on our SN 2020faa spectra in order to estimate the best comparison phase from that library of spectral templates. The results are shown in Fig. 7 where the estimated spectral age is plotted versus the actual age, showing that also (compare A17, their extended data fig. 4) SN 2020faa is slow evolving.

3.3. Bolometric lightcurve

In order to estimate a total luminosity, we attempted to construct a bolometric light curve and to estimate the total radiative energy output. We follow a similar Black-body (BB) approximation approach as done for iPTF14hls by A17, and for the early evolution probed here we have better photometric color coverage to pursue this.

The result is shown in Fig. 9. The red squares show the luminosity of iPTF14hls (from A17, their extended data fig. 2). There was only enough color information to fully construct this luminosity for iPTF14hls at later epochs. For SN 2020faa, we can use the *gri* coverage to estimate the luminosity also before this, and see that those estimates connect nicely at 150 days post discovery. Using this, we can estimate a maximum bolometric luminosity for SN 2020faa of $L_{bol} = 1.12 \times 10^{43}$ erg s^{-1} (at 120.55 rest frame days) and a total radiated energy over the first 124 rest frame days of $E_{rad} = 7.37 \times 10^{49}$ erg. This can be compared this to the total radiative output of iPTF14hls which was $E_{rad} = 3.59 \times 10^{50}$ erg over 1235 days (S19). In that paper, the early bolometric of iPTF14hls was reconstructed, and that comparison is also shown in Fig. 9. Within the uncertainties, these are quite similar, the S19 early bolometric luminosity was estimated from the *r*-band data and a constant bolometric correction. Already the first 150 days of SN 2020faa can not easily be powered by the mechanism usually responsible for a Type II SN lightcurve - radioactive decay. Using, $L = 1.45 \times 10^{43} exp(-\frac{t}{\tau_{Co}})(\frac{M_{Ni}}{M_{\odot}})$ erg s^{-1} from Nadyozhin (2003) implies that we would require more than a solar mass of ^{56}Ni to account for the energy budget. This is already out of the scope for the traditionally considered neutrino explosion mechanism (e.g., Terreran et al. 2017).

From the BB approximation we also obtain the temperature and the evolution of the BB radius. The radius evolution was an important clue to the nature of iPTF14hls in A17 (their fig. 4), and we therefore show a very similar plot in Fig. 10. The radius thus obtained is directly compared to the values for iPTF14hls and SN 1999em. We here also include the radius estimated from the spectroscopic velocities, estimated from the P-Cygni minima of the Fe ii λ5169 line. The figure shows that the BB radius of SN 2020faa at the earliest phases are similar and evolve similarly to those of SN 1999em, and approach the values of the radius for iPTF14hls at 140 days. The *vt* velocities on the other hand are higher for SN 2020faa, just as they were for iPTF14hls. We can see that they smoothly attach to the values for iPTF14hls.

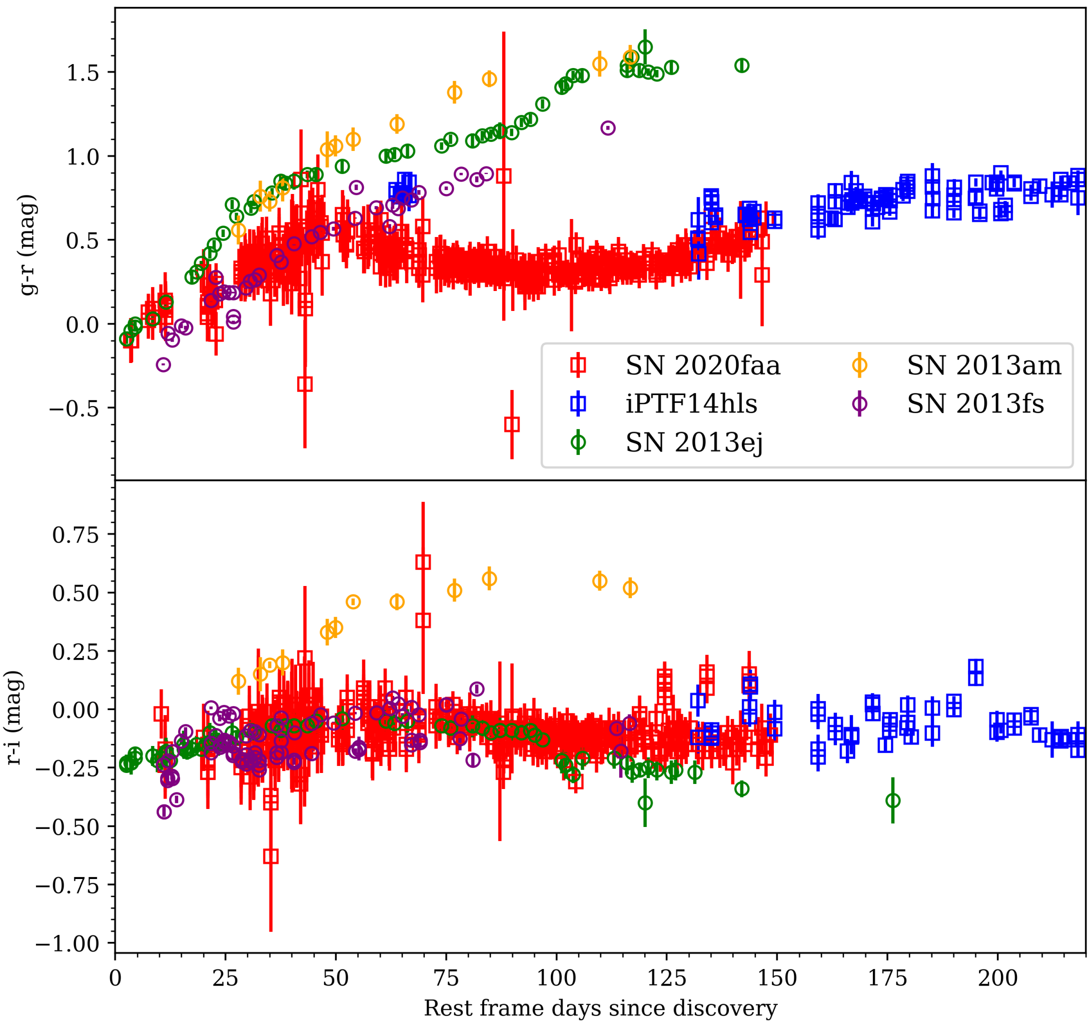

Fig. 5 Color evolution of SN 2020faa shown in $g - r$ (upper panel) and $r - i$ (lower panel). The colors have been corrected for MW extinction and are plotted in rest frame days relative to epoch of discovery. For comparison we have also plotted colors for iPTF14hls and for the normal Type II SNe 2013am, 2013fs and 2013ej. Their epochs for are also provided in rest frame days since discovery.

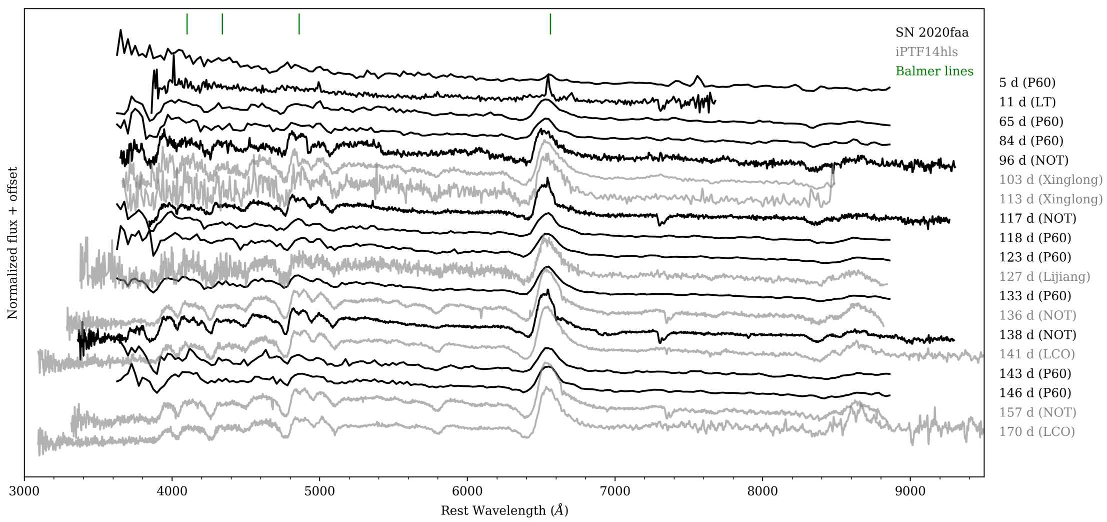

Fig. 6 Sequence of optical spectra for SN 2020faa. The complete log of spectra is provided in Table 1. The epoch of the spectrum is provided to the right. For comparison we also show spectra of iPTF14hls in grey.

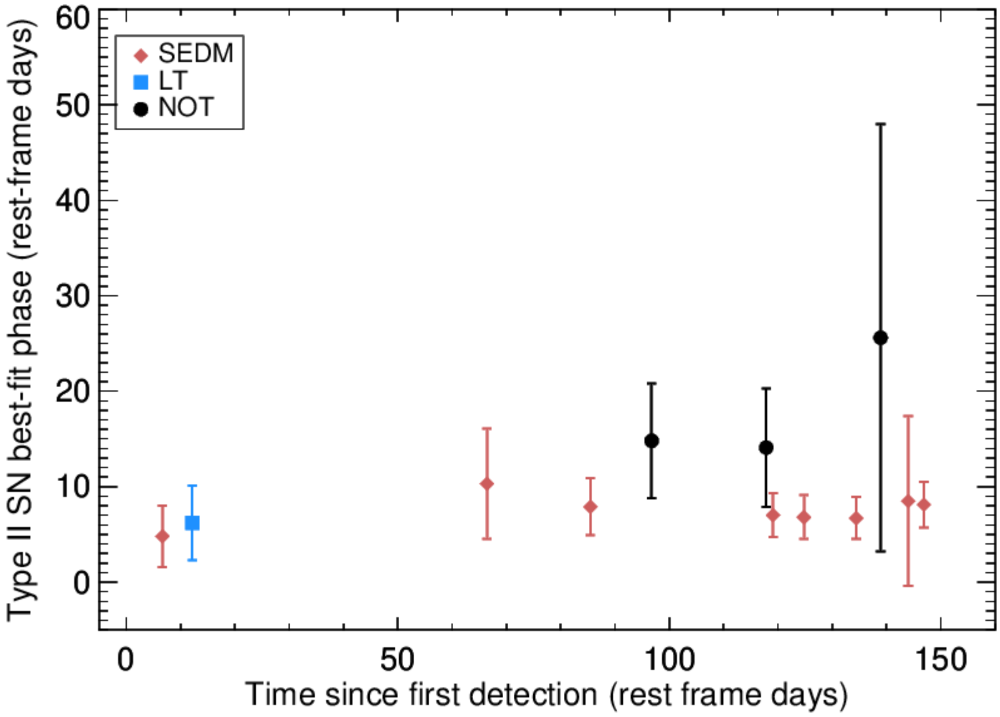

Fig. 7 Phases estimated by comparison to superfit templates are plotted versus rest fram days since first detection for SN 2020faa. The overall spectral evolution revealed by these comparisons is very slow and even at more than 100 days the best matches are with younger Type II SNe. This is similar to what was found by A17 for iPTF14hls, which consitued to display slow evolution for 600+ days.

3.4. Host galaxy

The results of the SED modeling of the host galaxy is displayed in Fig. 11. We obtain a good fit for a galaxy with a mass of $3.2{\times}10^9$ and a star-formation rate of 0.6 per year. This is a relatively regular host galaxy for a Type II SN. In Fig. 12 we compare the host mass with the distribution of host masses for SNe II from the PTF survey from Schulze et al. (2020). As can be seen, the host of SN 2020faa is a regular host galaxy in this respect, and is slightly more massive than the host for iPTF14hls, which is also illustrated in the figure.

4. Summary and Conclusions

We have presented SN 2020faa, a young sibling to the spectacular iPTF14hls. The first 150 days of the light curve evolution is very different from a normal Type II supernova, and very similar to that of iPTF14hls. We therefore encourage continued monitoring of this transient to explore if it will evolve in a similar fashion, with light curve undulations, longevity and a slow spectral evolution. From the observations already in hand, we can conclude that just as for iPTF14hls the energy budget is already too high to be driven by a standard radioactivity scenario. The plethora of other powering mechanism needs to be dusted off again, to explain the evolution of SN 2020faa.

ZTF will continue operations as ZTFII, with more discoveries in sight. Several community brokers are already processing the data in real time and more activity is foreseen as we come closer to the era of the Vera Rubin telescope. The broker `Alerce` (Förster et al. 2020) is an example where a combination of computer filtering and human inspection already provides early alerts for infant supernovae. We also need to keep an eye on supernova lightcurves that behave in unusual and interesting ways also at later stages. This includes re-brightenings as for SN 2020faa here or due to late CSM interaction as in Sollerman et al. (2020), but could also be rapid declines or undulations, as in iPTF14hls. Hitherto most of these have been found by human scanners reacting to a 'funny' light curve. This will unlikely be the case in the Rubin era.

Acknowledgements. Based on observations obtained with the Samuel Oschin Telescope 48-inch and the 60-inch Telescope at the Palomar Observatory as part of the Zwicky Transient Facility project. ZTF is supported by the National Science Foundation under Grant No. AST-1440341 and a collaboration including Caltech, IPAC, the Weizmann Institute for Science, the Oskar Klein Center at Stockholm University, the University of Maryland, the University of Washington, Deutsches Elektronen-Synchrotron and Humboldt University, Los Alamos National Laboratories, the TANGO Consortium of Taiwan, the University of Wisconsin at Milwaukee, and Lawrence Berkeley National Laboratories. Operations are conducted by COO, IPAC, and UW. The SED Machine is based upon work supported by the National Science Foundation under Grant No. 1106171. Partially based on observations made with the Nordic Optical Telescope, operated at the Observatorio del Roque de los Muchachos, La Palma, Spain, of the Instituto de Astrofisica de Canarias. Some of the data presented here were obtained with ALFOSC, which is provided by the Instituto de Astrofisica de Andalucia (IAA) under a joint agreement with the University of Copenhagen and NOTSA. S. Y. is funded through the GREAT research environment grant 2016-06012.

References

Ahn, C. P., Alexandroff, R., Allende Prieto, C., et al. 2014, ApJS, 211, 17
Andrews, J. E. & Smith, N. 2018, MNRAS, 477, 74

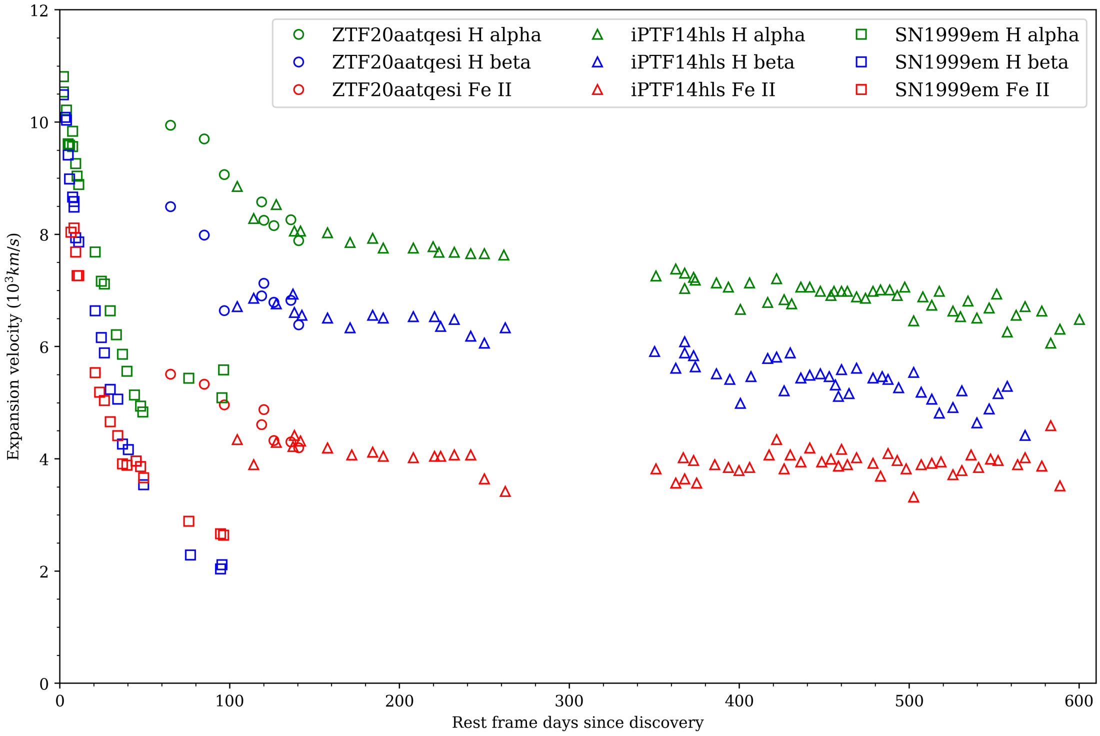

Fig. 8 Velocities estimated from the P-Cygni minima of Hα (green), Hβ (blue) and Fe II λ5169 (red) for the three SNe discussed throughout the paper. Whereas he normal Type II SN 1999em show a fast decline in expansion velocities, iPTF14hls exhibits virtually constant velocities, where the Fe velocity was lower than those estimated from Balmer lines at all epochs. For SN 2020faa we probe intermediate phases and see a slowing down of the photosphere, but with velocities very similar to those demonstrated by iPTF14hls at the common epochs around 150 days.

Arcavi, I., Howell, D. A., Kasen, D., et al. 2017, Nature, 551, 210
Bellm, E. C., Kulkarni, S. R., Graham, M. J., et al. 2019, PASP, 131, 018002
Blagorodnova, N., Neill, J. D., Walters, R., et al. 2018, PASP, 130, 035003
Bose, S., Sutaria, F., Kumar, B., et al. 2015, The Astrophysical Journal, 806, 160
Burrows, D. N., Hill, J. E., Nousek, J. A., et al. 2006, Space Science Reviews, 120, 165
Byler, N., Dalcanton, J. J., Conroy, C., & Johnson, B. D. 2017, ApJ, 840, 44
Calzetti, D., Armus, L., Bohlin, R. C., et al. 2000, ApJ, 533, 682
Cardelli, J. A., Clayton, G. C., & Mathis, J. S. 1989, ApJ, 345, 245
Cenko, S. B., Fox, D. B., Moon, D.-S., et al. 2006, PASP, 118, 1396
Chabrier, G. 2003, PASP, 115, 763
Chambers, K. C., Magnier, E. A., Metcalfe, N., et al. 2016, arXiv e-prints, arXiv:1612.05560
Chugai, N. N. 2018, Astronomy Letters, 44, 370
Conroy, C., Gunn, J. E., & White, M. 2009, ApJ, 699, 486
de Jaeger, T., Anderson, J. P., Galbany, L., et al. 2018, MNRAS, 476, 4592
Dekany, R., Smith, R. M., Riddle, R., et al. 2020, PASP, 132, 038001
Dessart. 2018, A&A, 610, L10
Dhungana, G., Kehoe, R., Vinko, J., et al. 2016, The Astrophysical Journal, 822, 6
Evans, P. A., Beardmore, A. P., Page, K. L., et al. 2009, MNRAS, 397, 1177
Evans, P. A., Beardmore, A. P., Page, K. L., et al. 2007, A&A, 469, 379
Foreman-Mackey, D., Sick, J., & Johnson, B. 2014, Python-Fsps: Python Bindings To Fsps (V0.1.1)
Förster, F., Cabrera-Vives, G., Castillo-Navarrete, E., et al. 2020, arXiv e-prints, arXiv:2008.03303
Fremling, C., Sollerman, J., Taddia, F., et al. 2016, A&A, 593, A68
Gehrels, N., Chincarini, G., Giommi, P., et al. 2004, ApJ, 611, 1005
Graham, M. J., Kulkarni, S. R., Bellm, E. C., et al. 2019, Publications of the Astronomical Society of the Pacific, 131, 078001
HI4PI Collaboration, Ben Bekhti, N., Flöer, L., et al. 2016, A&A, 594, A116
Huang, F., Wang, X., Zhang, J., et al. 2015, The Astrophysical Journal, 807, 59
Lang, D. 2014, AJ, 147, 108
Leja, J., Johnson, B. D., Conroy, C., van Dokkum, P. G., & Byler, N. 2017, ApJ, 837, 170
Mainzer, A., Bauer, J., Cutri, R. M., et al. 2014, ApJ, 792, 30
Martin, D. C., Fanson, J., Schiminovich, D., et al. 2005, ApJ, 619, L1
Masci, F. J., Laher, R. R., Rusholme, B., et al. 2019, PASP, 131, 018003
Mauerhan, J. C., Van Dyk, S. D., Johansson, J., et al. 2017, ApJ, 834, 118
Meisner, A. M., Lang, D., & Schlegel, D. J. 2017, AJ, 153, 38
Moriya, T. J., Mazzali, P. A., & Pian, E. 2019, Monthly Notices of the Royal Astronomical Society, 491, 1384
Nadyozhin, D. K. 2003, Monthly Notices of the Royal Astronomical Society, 346, 97
Perley, D. A., Taggart, K., Dahiwale, A., & Fremling, C. 2020, Transient Name Server Classification Report, 2020-987, 1
Rigault, M., Neill, J. D., Blagorodnova, N., et al. 2019, A&A, 627, A115
Roming, P. W. A., Kennedy, T. E., Mason, K. O., et al. 2005, Space Sci. Rev., 120, 95
Schulze, S., Yaron, O., Sollerman, J., et al. 2020, arXiv e-prints, arXiv:2008.05988
Skrutskie, M. F., Cutri, R. M., Stiening, R., et al. 2006, AJ, 131, 1163
Soker, N. & Gilkis, A. 2017, Monthly Notices of the Royal Astronomical Society, 475, 1198
Sollerman, J., Taddia, F., Arcavi, I., et al. 2019, A&A, 621, A30
Speagle, J. S. 2020, MNRAS, 493, 3132
Terreran, G., Pumo, M. L., Chen, T. W., et al. 2017, Nature Astronomy, 1, 713
Tomasella, L., Cappellaro, E., Pumo, M. L., et al. 2018, MNRAS, 475, 1937
Tonry, J., Denneau, L., Heinze, A., et al. 2020, Transient Name Server Discovery Report, 2020-869, 1
Valenti, S., Sand, D., Pastorello, A., et al. 2013, Monthly Notices of the Royal Astronomical Society: Letters, 438, L101
Wang, L. J., Wang, X. F., Wang, S. Q., et al. 2018, ApJ, 865, 95
Woosley, S. E. 2018, ApJ, 863, 105
Wright, A. H., Robotham, A. S. G., Bourne, N., et al. 2016, MNRAS, 460, 765
Wright, E. L., Eisenhardt, P. R. M., Mainzer, A. K., et al. 2010, AJ, 140, 1868
Yaron, O. & Gal-Yam, A. 2012, PASP, 124, 668
Yaron, O., Perley, D. A., Gal-Yam, A., et al. 2017, Nature Physics, 13, 510

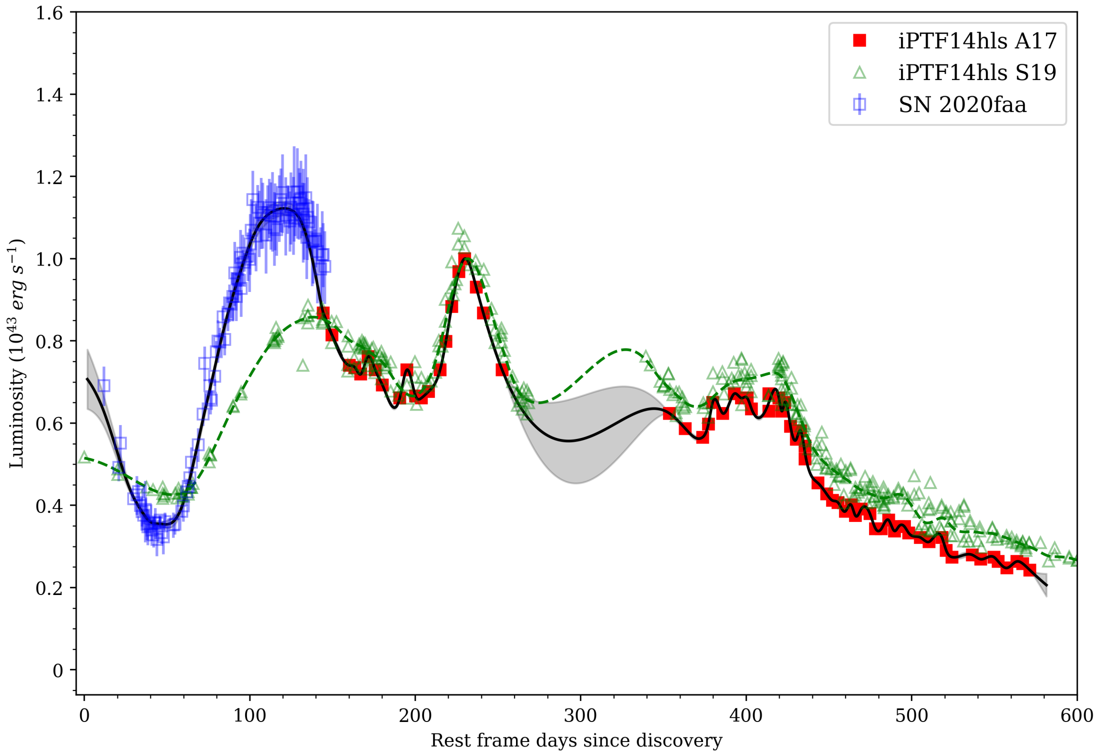

Fig. 9 Luminosity of SN 2020faa after accounting for MW extinction, distance and integrating a BB fit to the *gri* photometry. A similar method was used for iPTF14hls which only had color data past 150 days, and we can see that the early time emission of SN 2020faa nicely merges with the late time luminosity for iPTF14hls. The GP fit on the joint lightcurves of SN 2020faa and iPTF14hls is shown as a black line and grey error regions. In green is the luminosity estimate for iPTF14hls from S19, which assumed a constant bolometric correction at early times.

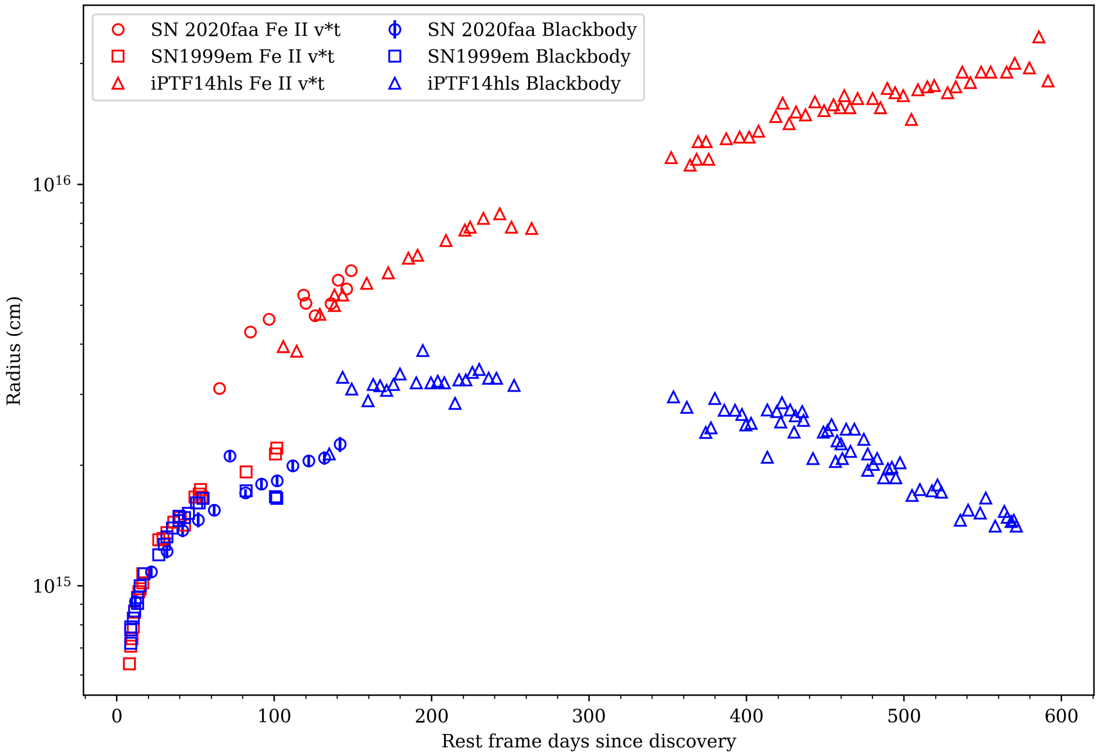

Fig. 10 Evolution of the the radius as a function of time for SN 2020faa (binned in 10 days), as compared to the extraordinary iPTF14hls and the regular Type II SN 1999em. This figure closely follows the presentation from A17, their fig. 4, and shows estimates for the radius evolution from two different methods for the three different SNe. A main theme in A17 was that for iPTF14hls, the radius evolution estimated from the BB approximation and the radius estimated from the spectroscopic velocities were different and diverged with time.

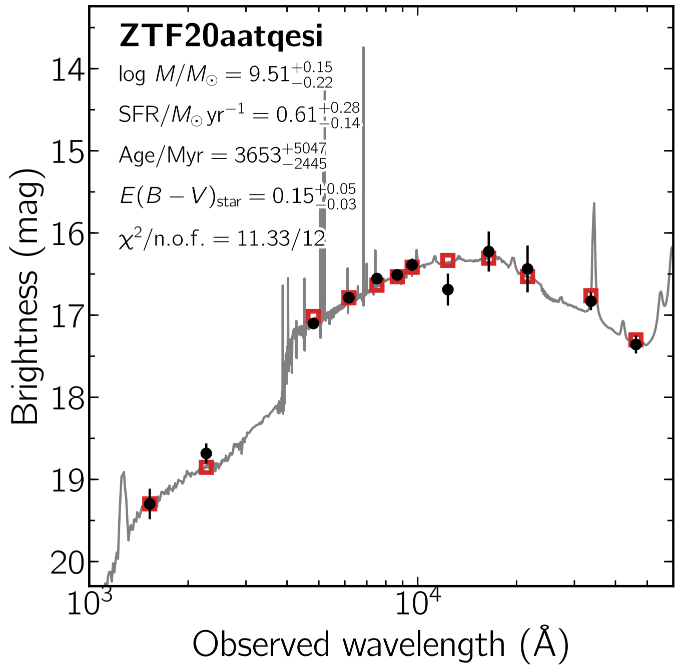

Fig. 11 Spectral energy distribution of the host galaxy of SN 2020faa from 1000 to 60,000 Å (black data points). The solid line displays the best-fitting model of the SED. The red squares represent the model-predicted magnitudes. The fitting parameters are shown in the upper-left corner. The abbreviation "n.o.f." stands for numbers of filters.

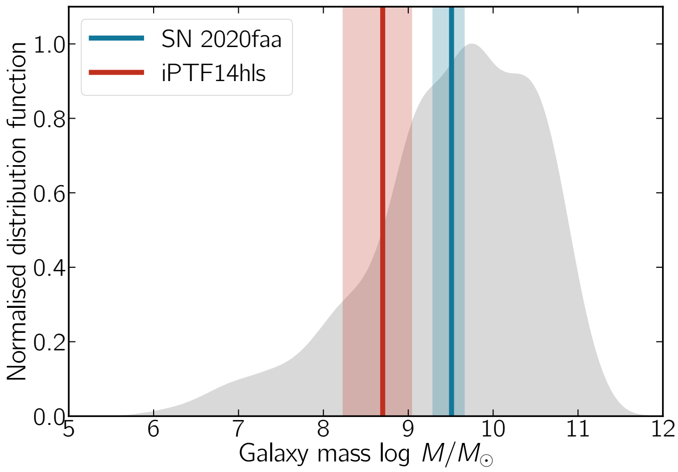

Fig. 12 The host-galaxy mass of SN 2020faa and iPTF14hls in the context of SNe II from the PTF and iPTF survey (as presented by Schulze et al. (2020)).

Table 1. Summary of Spectroscopic Observations

Object	Observation Date (YYYY MM DD)	Phase (Rest-frame days)	Telescope+Instrument
SN 2020faa	2020 Mar 31	6.7	P60+SEDM
SN 2020faa	2020 Apr 05	12.4	LT+SPRAT
SN 2020faa	2020 Jun 01	68.8	P60+SEDM
SN 2020faa	2020 Jun 21	88.7	P60+SEDM
SN 2020faa	2020 Jul 02	100.4	NOT+ALFOSC
SN 2020faa	2020 Jul 24	122.4	NOT+ALFOSC
SN 2020faa	2020 Jul 26	123.7	P60+SEDM
SN 2020faa	2020 Aug 01	129.6	P60+SEDM
SN 2020faa	2020 Aug 11	139.6	P60+SEDM
SN 2020faa	2020 Aug 15	144.3	NOT+ALFOSC
SN 2020faa	2020 Aug 21	149.6	P60+SEDM
SN 2020faa	2020 Aug 24	152.6	P60+SEDM

Table 2. Host galaxy photometry

Survey	Filter	Wavelength	Brightness
GALEX	FUV	1549.0	19.30 ± 0.16
GALEX	NUV	2304.7	18.68 ± 0.07
PS1	g	4810.9	17.10 ± 0.03
PS1	r	6156.4	16.79 ± 0.03
PS1	i	7503.7	16.56 ± 0.03
PS1	z	8668.6	16.51 ± 0.03
PS1	y	9613.5	16.39 ± 0.06
2MASS	J	12350	16.69 ± 0.19
2MASS	H	16620	16.23 ± 0.24
2MASS	K	21590	16.44 ± 0.27
WISE	$W1$	33526	16.83 ± 0.04
WISE	$W2$	46028	17.36 ± 0.04

Note. — All measurements are reported in the AB system and are not corrected for extinction. The effective wavelengths of the filter response functions were taken from http://svo2.cab.inta-csic.es/theory/fps/.